

RESEARCH PAPER

OPEN ACCESS 

# Identification of potential biomarkers and immune cell infiltration in acute myocardial infarction (AMI) using bioinformatics strategy

Yun Xie, Yi Wang, Linjun Zhao, Fang Wang, and Jinyan Fang 

Department of Emergency, Affiliated Hangzhou First People's Hospital, Zhejiang University School of Medicine, Hangzhou, Zhejiang, China

## ABSTRACT

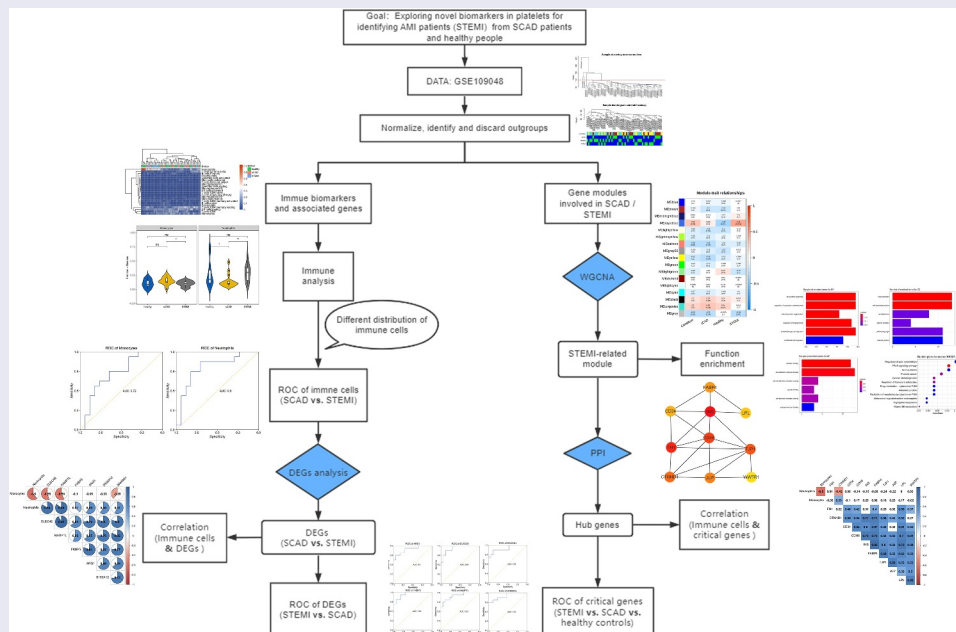
Acute myocardial infarction (AMI) was considered a fatal disease resulting in high morbidity and mortality; platelet activation or aggregation plays a critical role in participating in the pathogenesis of AMI. The current study aimed to reveal the underlying mechanisms of platelets in the confrontation of AMI and potential biomarkers that separate AMI from other cardiovascular diseases and healthy people with bioinformatic strategies. Immunity analysis revealed that the neutrophil was significantly decreased in patients with SCAD compared with patients with ST-segment elevation myocardial infarction (STEMI) or healthy controls; monocytes and neutrophils showed potential in distinguishing patients with STEMI from patients with SCAD. Six differentially expressed genes (DEGs) showed great performances in differentiating STEMI patients from SCAD patients with AUC greater than 0.9. Correlation analysis showed that these six DEGs were significantly positively correlated with neutrophils; three genes were negatively correlated with monocytes. Weighted gene co-expression network analysis (WGCNA) found that module 'royal-blue' had the highest correlation with STEMI; genes in STEMI-related module were enriched in cell–cell interactions, blood vessels' biological processes, and peroxisome proliferator-activated receptor (PPAR) signaling pathway; four genes (*FN1*, *CD34*, *LPL*, and *WWTR1*) represented the capability of identifying patients with STEMI from healthy controls and patients with SCAD; two genes (*ARG1* and *NAMPTL*) were considered as novel biomarkers for identifying STEMI from SCAD; *FN1* represented the potential as a novel biomarker for STEMI. Our findings indicated that the distribution of neutrophils could be considered as a potential molecular trait for separating patients with STEMI from SCAD.

## ARTICLE HISTORY

Received 21 April 2021  
Revised 28 May 2021  
Accepted 29 May 2021

## KEYWORDS

Neutrophils; STEMI; scad; *arg1*; *namptl*; *fn1*



**CONTACT** Jinyan Fang  [fjy830818@126.com](mailto:fjy830818@126.com)  Department of Emergency, Affiliated Hangzhou First People's Hospital, Zhejiang University School of Medicine, NO 261 HuanSha Road, Hangzhou, Zhejiang, 310006, China

© 2021 The Author(s). Published by Informa UK Limited, trading as Taylor & Francis Group. This is an Open Access article distributed under the terms of the Creative Commons Attribution-NonCommercial License (<http://creativecommons.org/licenses/by-nc/4.0/>), which permits unrestricted non-commercial use, distribution, and reproduction in any medium, provided the original work is properly cited.

## Introduction

Acute myocardial infarction (AMI) remains one of the leading reasons for morbidity and mortality worldwide, despite the improvements in prognosis and therapy. Early and accurate diagnoses can guarantee immediate medical care, thus reducing the death rate and enhancing prognoses [1]. AMI is an event of ischemic myocardial necrosis, caused by an acute interruption of myocardial blood flow [2]. It is a subgroup of acute coronary syndromes and can be divided into ST-segment elevation myocardial infarction (STEMI) or non-ST-elevation myocardial infarction (NSTEMI) [3]. Cardiac troponin T (cTn), I or T, is considered as a gold standard biomarker for AMI; the unconventionally increase of cTn, however, generally refers to myocardial necrosis which might be caused by other diseases such as heart failure, myocarditis, and chest trauma, while renal failure may also lead to increased cTnI [4]. There is an urgent need for new biomarkers, especially molecular features with high sensitivity and specificity in the early stages of AMI, to narrow the diagnostic period and boost the outcome of patients with AMI.

Platelets, containing nuclei and RNAs, maintain a strong presence in mediating the genesis and progression of atherosclerosis; multiple genes involved in platelets have been reported to be associated with coronary artery disease [5,6]. Platelet activation is characteristic of acute coronary syndromes (ACSs) caused by coronary atherosclerotic plaque rupture or thrombogenic substances exposure, contributing to the construction of intraluminal thrombus, and thus reducing coronary blood flow [7]. Neutrophils are the most abundant circulating leucocytes in healthy people and the first immune cells during infection or injury [8]. AMI causes a sterile inflammatory response, and neutrophils have been reported to play a vital role in the process of myocardial inflammation [9]. The previous research showed that neutrophil-derived S100A8/A9 could amplify granulopoiesis after myocardial infarction (MI) [10]. A calcium-sensing receptor on neutrophil promoted myocardial apoptosis and fibrosis via NLRP3 inflammasome activation after AMI [11]. The compromised anti-inflammatory action of neutrophil extracellular traps in PAD4-Deficient

mice aggravated acute inflammation after MI [12]. Neutrophils were involved in post-MI cardiac repair through polarizing macrophages to a reparative phenotype [13]. Analysis of the proportion of immune states of platelets and molecular changes of platelets in patients with AMI, compared with other cardiovascular diseases (CVDs), such as stable coronary artery diseases (SCAD), was limited.

In this study, we aimed to analyze immune cell changes and explore novel biomarkers in platelets associated STEMI with expression profiles of blood platelets from the Gene Expression Omnibus (GEO) database. Immune cell fractions from patients with different cardiovascular diseases (STEMI and SCAD, in this study) and healthy donors were analyzed; correlation analysis between genes and immune cells was performed. Functional enrichment analysis and protein–protein interactions (PPI) predictions of genes involved in STEMI-related module identified by WGCNA were performed to explore molecular changes of platelets and critical genes, respectively. The receiver operating characteristic (ROC) curves and principal component analysis (PCA) were analyzed and depicted for diagnostic value analysis.

## Methods and materials

### Data collecting and processing

We downloaded an expression data GSE109048 from GEO (<https://www.ncbi.nlm.nih.gov/geo/>). Platelet gene expression profiling GSE109048 contains 19 STEMI patients, 19 healthy donors (HD), and 19 SCAD patients. According to the [HTA-2\_0] Affymetrix Human Transcriptome Array 2.0 [transcript (gene) version] platform, probes were converted into the corresponding gene symbols. The data were normalized using the *limma* package for further analysis [14]. A clustering tree of samples was constructed with expression, the outliers were observed and discarded.

### Immune infiltration analysis

The immune infiltration analysis was performed to illustrate the correlation between immune cell

distribution and AMI compared with patients with SCAD and healthy donors. The fractions of 22 immune cells were detected using a web-based tool CIBERSORTx (<https://cibersortx.stanford.edu/>), which can estimate the abundance of member cell types in a mixed cell population. The samples were divided into three groups: healthy individuals, SCAD, and STEMI based on disease conditions obtained from the clinical information; the proportion of immune cells was visualized and depicted using a heatmap. Immune cells with obvious variety among samples were visualized using violin plots; distributions of immune cells among different groups were compared and estimated using a *T*-test.

### **ROC analysis of immune cells and DEGs**

To evaluate the diagnostic value of immune cells, ROC analysis and PCA were conducted and portrayed. To obtain the DEGs in different groups, we conducted DEGs analysis with normalized expression data of trimmed samples after clustering; adjusted *P*-value <0.05 were set as the cutoff to identify significantly differentially expressed genes.

### **Correlation analysis of DEGs and immune cells**

Correlation between DEGs and fractions of immune cells was conducted to explore DEGs associated with immune cells (with different proportions among different groups). The scores and significance of the correlation were calculated using the Pearson method; correlation matrix of DEGs and immune cells selected was depicted using a heatmap; background color of correlation without significance ( $P > 0.01$ ) was blanked.

### **WGCNA analysis**

To explore the clinical traits-related modules and genes related to SCAD and AMI, the R package WGCNA was performed [15]. The mean connectivity and scale independence function as soft threshold were calculated and visualized to choose the optimal power value for network construction. The adjacency matrix was converted into a topological overlap matrix (TOM) with a suitable power value. Genes were classified into

different modules based on the TOM; modules with significant similarity (correlation >0.75) were merged. Correlation between modules and clinical traits was calculated and depicted; genes in the most significantly AMI-related modules were selected for further analysis.

### **Function analysis of crucial modules**

To examine the molecular process or critical pathways of genes from crucial modules associated with AMI, functional enrichment analysis was performed using an R package clusterProfiler [16]. Genes were converted into 'ENTREZID' and 'UNIPROT' format for GO and KEGG analyses, respectively. The minimum GO and KEGG term size of annotated genes was set to 10. Both *P* and *Q* values were set to 0.05 for significant enriched terms analysis.

### **PPI analysis of critical modules**

The online database STRING (<https://string-db.org/>) was used to predict the interaction networks of protein-protein. Cytoscape software (<https://cytoscape.org/>) was used to visualize the PPI; crucial genes were predicted and ranked with Cytoscape with interactions among proteins; top 10 critical genes were selected as hub genes for this analysis; the rank and interactions of hub genes were color-coded visualized with Cytoscape. ROC analysis was performed to evaluate the diagnostic value of hub genes for patients with STEMI; the correlation between critical genes and the proportion of immune cells was analyzed. The expression of critical genes, DEGs, and immune cells were fitted by Gene Set Variation Analysis (GSVA) [17]; the potential of the GSVA index as a diagnostic biomarker for distinguishing patients with STEMI was estimated via ROC analysis.

### **Statistical analysis**

The significance of DEGs was evaluated with the limma package [14]. Correlation between modules and clinical traits was performed with WGCNA package [15]; the significance of enrichment of genes in function enrichment analysis was tested with clusterProfiler package [16]; the correlation

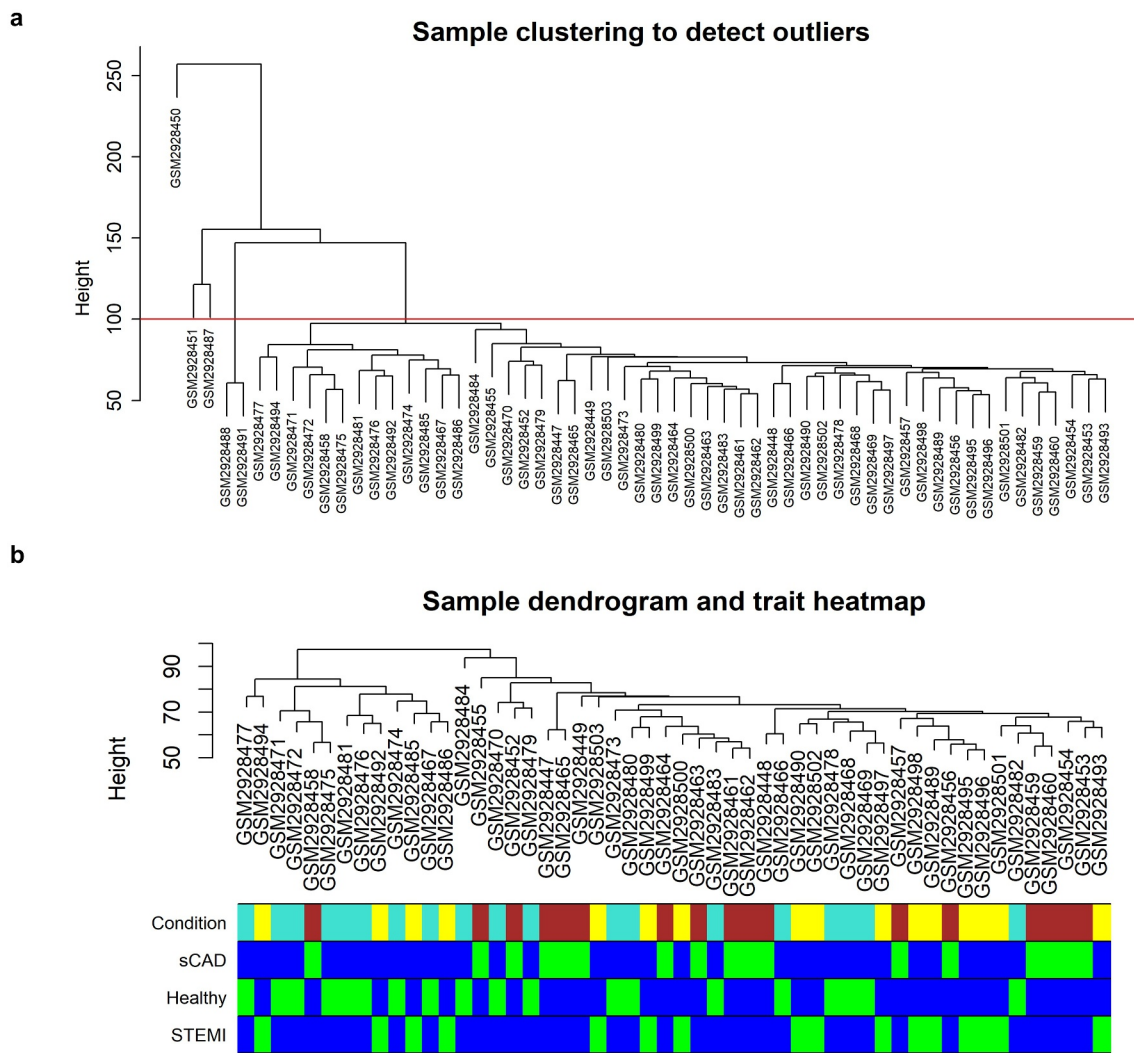


**Figure 1. Clustering dendrogram of GSE109048.** (a) A clustering tree of samples was constructed with expression; cutoff for outgroups was depicted with a red line. (b) The associated clinical traits were mapped to the clustering tree without outgroups.

between genes expression and immune cells fraction were calculated using the Pearson method and test with *T*-test method in R package.

## Results

### *Immune cells associated with AMI and CAD*

Based on the clustering dendrogram, five outliers (two SCAD samples and three STEMI samples) were observed and discarded (Figure 1a); 52 samples including 16 patients with STEMI, 17 patients with SCAD, and 19 healthy controls were finally utilized for this study; the color-coded clinical traits were mapped to the clustering dendrogram constructed on the samples without outgroups (Figure 1b).

The platelet activation or aggregation participates in a crucial role in the pathogenesis of AMI; immunity analysis was performed to analyze immune cell fractions among these three groups; fractions of 22 type immune cells were visualized with a heatmap (Figure 2a). We observed different distributions of immune cells, such as neutrophils, T cells CD4 memory resting, NK cells resting, and monocytes among samples (Figure 2a). We compared the distribution of immune cells in the three groups (STEMI vs. SCAD, STEMI vs. healthy, SCAD vs. healthy) using a *T*-test and obtained a significant difference in the proportion of monocytes between STEMI and SCAD patients; no obvious difference was observed in disease (STEMI and SCAD) groups and healthy controls (Figure 2b). Neutrophils were significantly

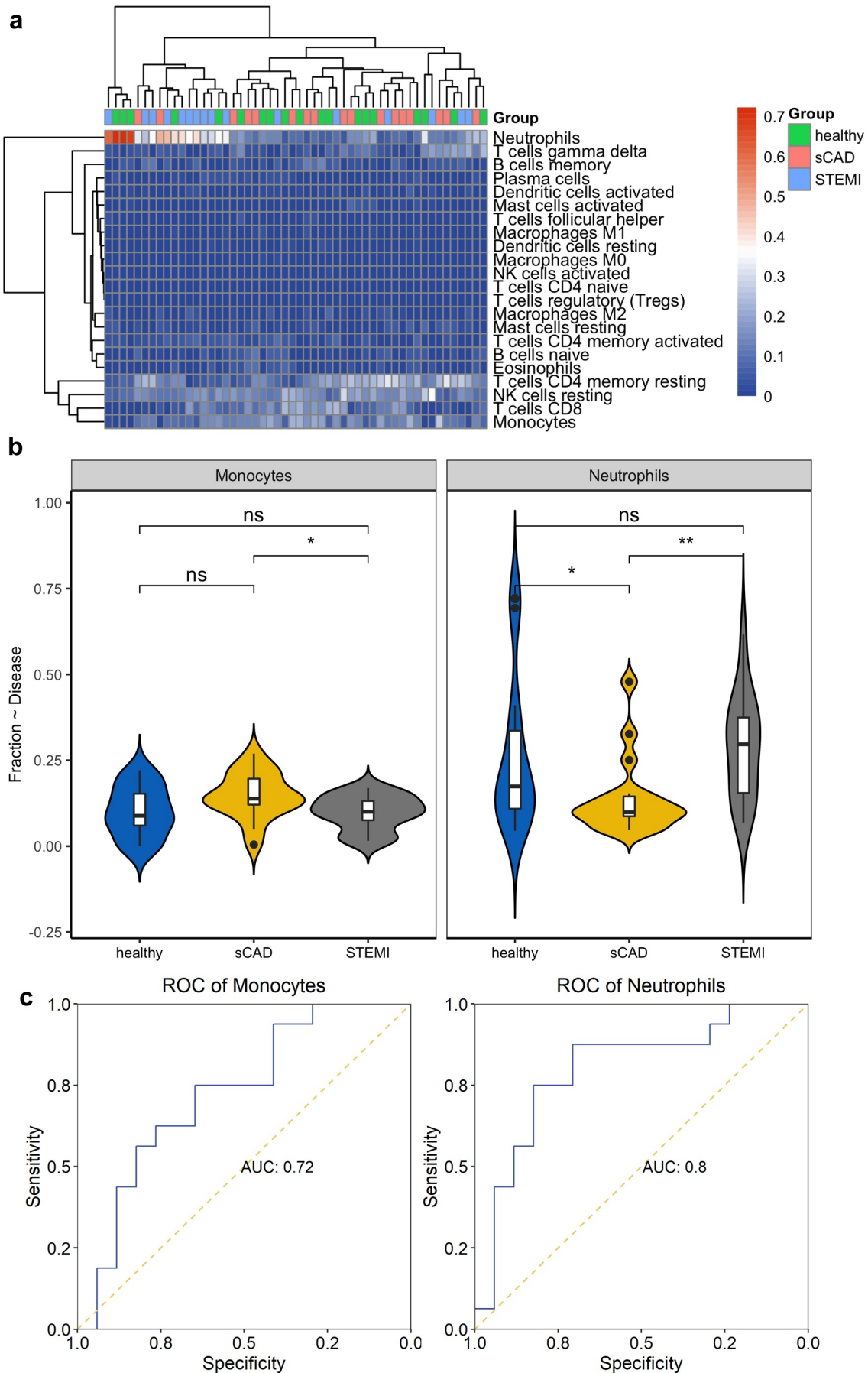


**Figure 2. Immune cell distribution among the three groups.** (a) Heatmap was constructed to depict the distribution of immune cells among samples. (b) Comparison of immune cells in the three groups was visualized with violin plots. (c) The capability of immune cells in identifying patients with STEMI was shown using ROC plots.

decreased in patients with SCAD compared with patients with STEMI or healthy controls; compared with the healthy group, neutrophils distribution showed no significant difference in patients with STEMI (Figure 2b). These two immune cells indicated potential (monocytes of AUC 0.72 and neutrophils of AUC 0.8) to separate patients with STEMI from patients with SCAD (Figure 2c).

### **DEGs involved in STEMI and SCAD**

Considering the observation of the immune difference between patients with SCAD and patients with STEMI, we further analyzed differentially expressed genes in 16 STEMI patients compared with 17 SCAD patients. We obtained six DEGs: *ARG1*, *CLEC4E*, *FKBP5*, *NAMPTL*, *S100A12*, and *SAMSN1* with an adjusted *P*-value <0.05. ROC results showed all DEGs had great performances (*ARG1* with AUC of 0.9, *CLEC4E* with AUC of 0.94, *FKBP5* with AUC of 0.95, *NAMPTL* with AUC of 0.92, *S100A12* with AUC of 0.92, and *SAMSN1* with AUC of 0.92) in classifying patients with STEMI from patients with SCAD (Figure 3a). Correlation of DEGs and fraction of two immune cells (neutrophils and monocytes) was analyzed; we observed a significant positive correlation between neutrophils and expressions of six DEGs (Figure 3b); two of these genes (*CLEC4E* and *NAMPTL*) indicated a relatively high correlation (0.84 and 0.85, respectively); expression of three genes (*CLEC4E*, *NAMPTL*, and *SAMSN1*) showed a significant negative correlation with the distribution of monocytes (Figure 3b). We performed PCA using the expression of *CLEC4E* and *NAMPTL* with the distribution of neutrophils and observed their good performance in separating STEMI from SCAD patients (Figure 3c).

### **Critical modules associated with STEMI**

To analyze gene modules (clusters) associated with AMI, we conducted gene expression networks with WGCNA. From mean connectivity and scale independence plots, we selected  $\beta = 6$  as the power value for network construction (Figure 4a, 4b). A total of 16 modules were observed from WGCNA, including ‘black’ with 1365 genes, ‘blue’ with 7282 genes, ‘brown’ with 5089 genes,

‘cyan’ with 336 genes, ‘darkred’ with 88 genes, ‘green’ with 2075 genes, ‘greenyellow’ with 3583 genes, ‘grey60’ with 802 genes, ‘lightcyan’ with 256 genes, ‘lightgreen’ with 1226 genes, ‘lightyellow’ with 141 genes, ‘midnightblue’ with 295 genes, ‘royalblue’ with 141 genes, ‘salmon’ with 555 genes, ‘turquoise’ with 7374 genes, and ‘yellow’ with 2857 genes (Figure 4c, 4d). Genes in module ‘royalblue’ indicated a high correlation with STEMI (cor = 0.44, *p* = 0.001) (Figure 4e). Module membership showed a significant correlation with gene significance (Figure 4f); the correlation of genes and modules was depicted (Figure 4g).

### **Functional analysis of genes in STEMI-related modules**

Functional enrichment of clinically significant modules, containing 141 genes, showed that 55 GO terms including 34 terms in biological process (BP), 13 in cellular component (CC), and 8 in molecular function (MF) were significantly enriched (Figure 5a,b,c, Table 1). GO terms were enriched in cell–cell interactions such as junction and adhesion and cell migration, locomotion, and motility (GO:0030336, GO:0040013, and GO:2000146). Biological processes associated with blood vessels such as regulation of vasculature development (GO:1901342) and angiogenesis (GO:0045765) were significantly enriched (Figure 5a, Table 1). Thirteen KEGG pathways were enriched with genes in STEMI-associated modules; KEGG enrichment analysis showed that genes focused on the regulation of actin cytoskeleton, a pathway that regulates cell motility and cell shape in cell cycles or response to extracellular stimuli (Figure 5d, Table 2). One crucial pathway mediating the cardiac energy metabolism – peroxisome proliferator-activated receptor (PPAR) signaling pathway (Figure 5d); two cytochrome P450-related pathways (hsa00980 and hsa00982) were significantly enriched (Figure 5d, Table 2).

### **Critical genes in STEMI-associated modules**

Protein–protein interactions analysis was a powerful strategy to explore critical and hub genes. Via analyzing protein–protein interactions

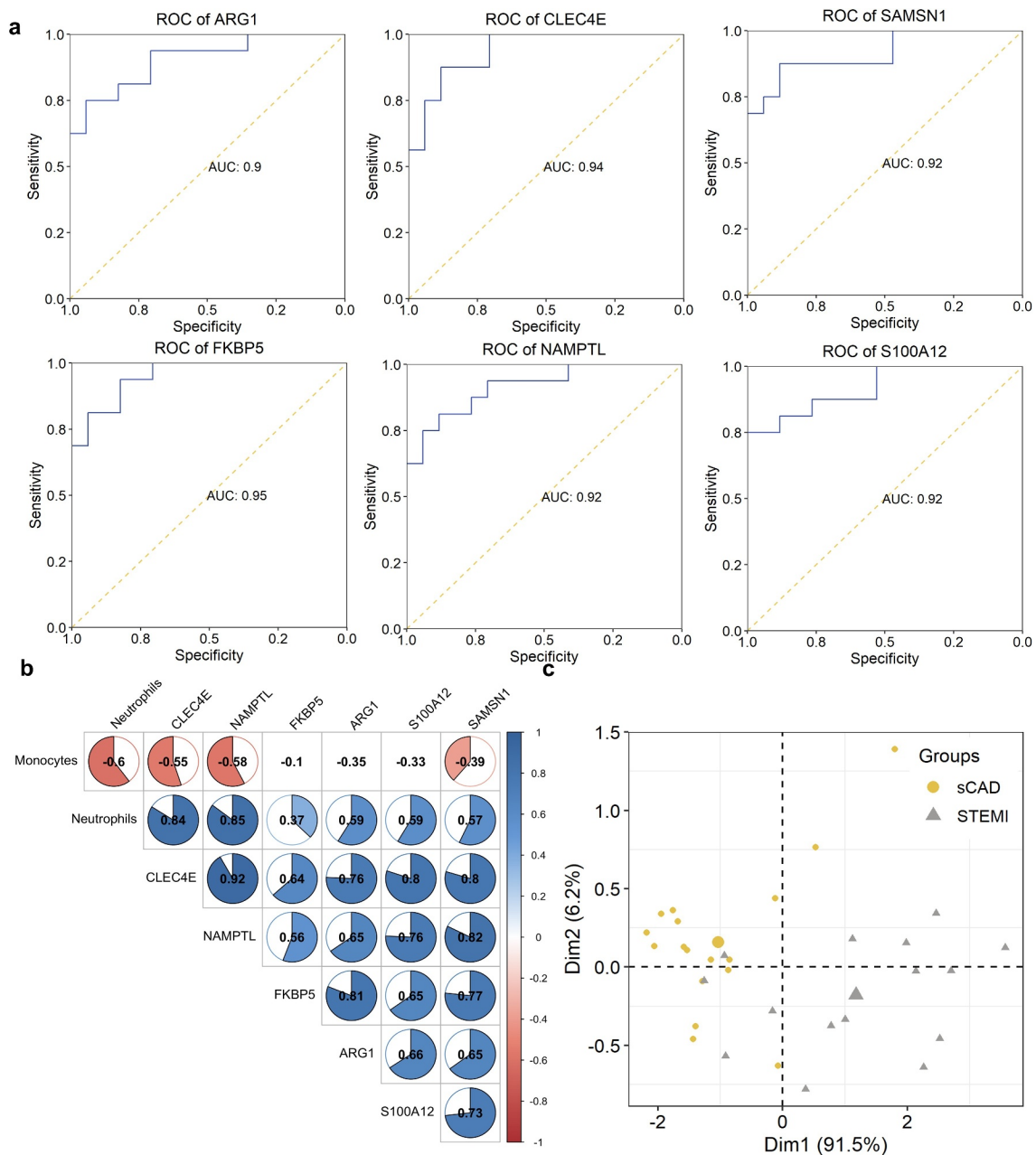


**Figure 3. ROC and correlation analysis of DEGs.** (a) ROC analysis of DEGs in identifying patients with STEMI. The potential of DEGs in separating patients with STEMI from SCAD. (b) Correlation between DEGs and immune cell distribution. The diagram visualized the correlation matrix of DEGs, neutrophils, and monocytes distribution; the correlation was represented with color from  $-1$  (red) to  $1$  (blue); blank boxes indicated the correlation was not significant ( $P > 0.01$ ); (c) PCA with the expression of *CLEC4E* and *NAMPTL* and neutrophils distribution.

among genes in module ‘royalblue’ and predicting crucial genes with Cytoscape software, we obtained 10 hub genes: *INS*, *FN1*, *CDH5*, *TJP1*, *CTNND1*, *JUP*, *FABP4*, *CD34*, *LPL*, and *WWTR1* (Figure 6).

Eight genes (*INS*, *FN1*, *CDH5*, *TJP1*, *FABP4*, *CD34*, *LPL*, and *WWTR1*) showed potential in

separating patients with STEMI from healthy controls with AUC higher than 0.7 (Figure 7). Four genes (*FN1*, *CD34*, *LPL*, and *WWTR1*) represented capability in identifying patients with STEMI from patients with SCAD with AUC  $> 0.7$  (Figure 8). We observed expression of one gene – *FN1* – showed great performance in identifying patients

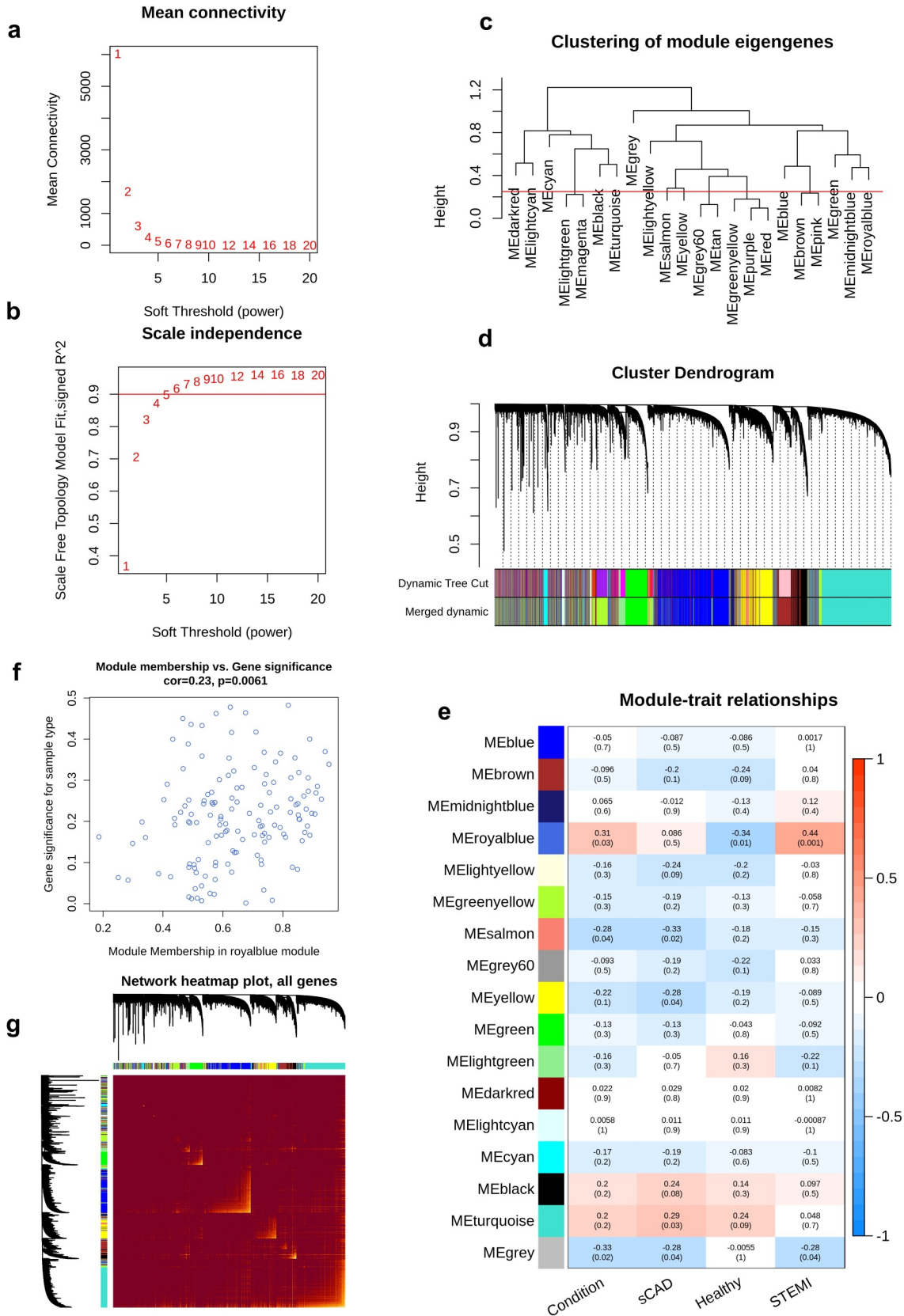


**Figure 4. WGCNA analysis of STEMI.** The mean connectivity and scale independence value as a function of soft threshold (power) were depicted (a, b); the red line indicated the cutoff of scale independence of 0.9. (c) Clustering dendrogram of modules; red line indicates the threshold of merging modules. (d) Modules before or after merging and clustering. (e) The heatmap depicted the correlation scores (digit in the box above) as well as its corresponding *P*-value (digit in the box below) of modules (rows) and clinical traits (columns). The correlation of module membership and gene significance, as well as the correlation among all genes, were visualized in (f) and (g).

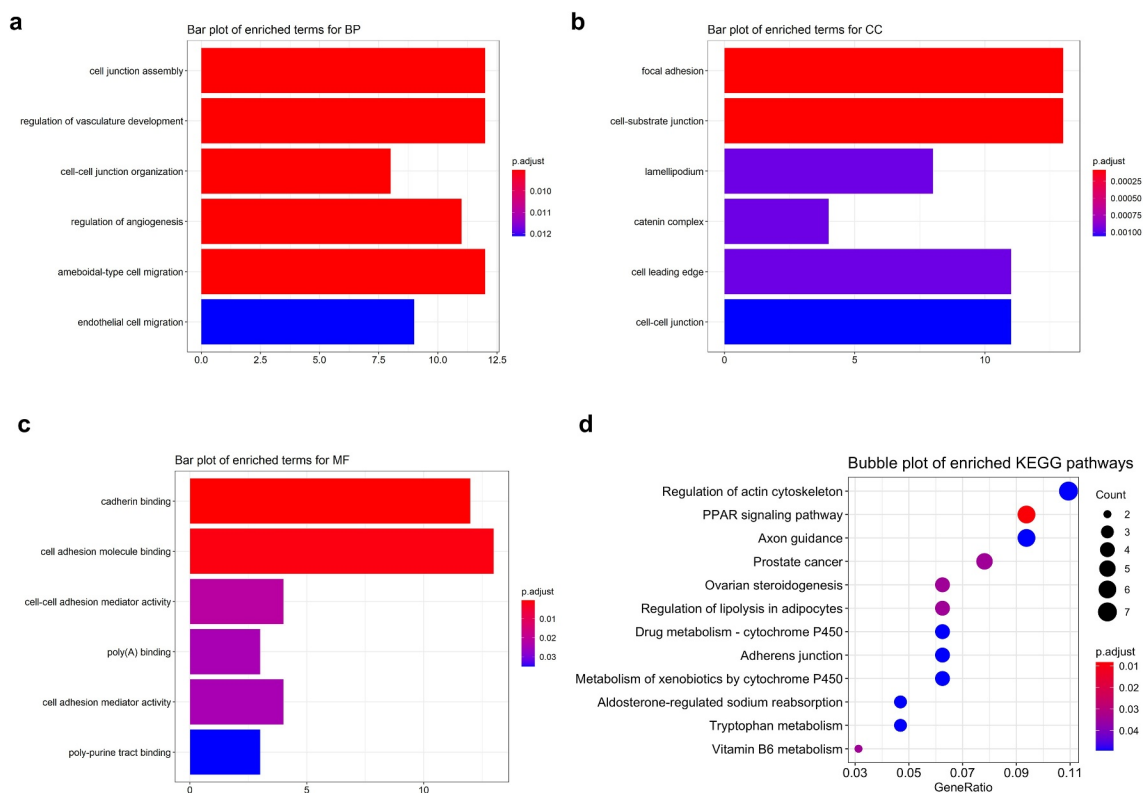


**Figure 5. Functional enrichment of STEMI-related genes.** Top 6 enriched GO terms in biological process (BP), cellular component (CC), and molecular function (MF) were depicted with bar plots (a, b, c); top 12 enriched KEGG pathways were visualized with bubble plots (d).

with STEMI from patients with SCAD (with AUC of 0.85 showed in Figure 8b) and healthy controls with AUC of 0.9 (Figure 7b).

We performed a correlation analysis to explore the association of hub genes expression and distribution of neutrophils and monocytes; almost all of the hub genes represented no relation with fractions of these two types of immune cells, except for a slight correlation for *CTNND1* (Figure 9a). Hub genes showed a significant positive correlation with each other, suggesting their potential in forming gene modules (Figure 9a). When constructing the GSVA indices of *ARG1*, *NAMPTL*, and *FNI* expression and neutrophils distribution, we found they showed great performance in identifying patients with STEMI from SCAD with an AUC of 0.95 (Figure 9b).

## Discussion

Considering the different proportion of monocytes and neutrophils between STEMI and SCAD

(Figure 2b), we further explored DEGs associated with immune cells in two disease groups. Six DEGs (*ARG1*, *CLEC4E*, *SAMSNI*, *FKBP5*, *NAMPTL*, and *S100A12*) were obtained, all of which indicated great performance in identifying patients with STEMI from SCAD with AUC > 0.9 (Figure 3a). However, we noticed differences in our research compared with the previous study, which observed five differentially expressed genes *FKBP5*, *S100P*, *SAMSNI*, *CLEC4E*, and *S100A12* [17–26]; we observed two additional novel DEGs *ARG1* and *NAMPTL*; different expression of *S100P* among STEMI and SCAD was failed to be observed in our study. This variety was caused by various preprocessing of the expression data: in our analysis, before DEGs analysis, we performed clustering with gene expression to identify experimentally caused outliers and discarded five samples including three patients with STEMI and 2 with SCAD (Figure 1a). A recent publication reported the significantly increased expression of

**Table 1.** GO enrichment terms of genes associated with AMI.

ONTOLOGY	ID	Description	p.adjust	qvalue	geneID
BP	GO:0034329	cell junction assembly	0.009006759	0.008184047	LIMS2, FN1, FAM107A, EFNA5, NRP1, CTNND1, FERMT2, TJP1, CDH5, CDH13, GJC1, JUP
BP	GO:1,901,342	regulation of vasculature development	0.009006759	0.008184047	CD34, CYP1B1, PLK2, ECSCR, SASH1, MEOX2, HEY1, DAB2IP, NRP1, CDH5, JUP, PTPRM
BP	GO:0045216	cell-cell junction organization	0.009006759	0.008184047	LIMS2, CTNND1, RASSF8, TJP1, CDH5, CDH13, GJC1, JUP
BP	GO:0045765	regulation of angiogenesis	0.009006759	0.008184047	CD34, CYP1B1, PLK2, ECSCR, SASH1, MEOX2, DAB2IP, NRP1, CDH5, JUP, PTPRM
BP	GO:0001667	ameboidal-type cell migration	0.009006759	0.008184047	CYP1B1, FN1, PLK2, SASH1, MEOX2, DAB2IP, NRP1, EDNRB, CDH13, KRT16, JUP, PTPRM
BP	GO:0043542	endothelial cell migration	0.012115814	0.011009109	CYP1B1, PLK2, SASH1, MEOX2, DAB2IP, NRP1, CDH13, JUP, PTPRM
BP	GO:0034332	adherens junction organization	0.012115814	0.011009109	CTNND1, RASSF8, CDH5, CDH13, JUP
BP	GO:0010631	epithelial cell migration	0.012115814	0.011009109	CYP1B1, PLK2, SASH1, MEOX2, DAB2IP, NRP1, CDH13, KRT16, JUP, PTPRM
BP	GO:0090132	epithelium migration	0.012115814	0.011009109	CYP1B1, PLK2, SASH1, MEOX2, DAB2IP, NRP1, CDH13, KRT16, JUP, PTPRM
BP	GO:0090130	tissue migration	0.012115814	0.011009109	CYP1B1, PLK2, SASH1, MEOX2, DAB2IP, NRP1, CDH13, KRT16, JUP, PTPRM
BP	GO:0007160	cell-matrix adhesion	0.012115814	0.011009109	CD34, FN1, FAM107A, EFNA5, NRP1, FERMT2, CDH13, JUP
BP	GO:0090136	epithelial cell-cell adhesion	0.015809313	0.014365229	CYP1B1, JUP, SERPINB8
BP	GO:0040013	negative regulation of locomotion	0.015814018	0.014369505	CYP1B1, IGFBP5, DPYSL3, MEOX2, DAB2IP, NRP1, DACH1, KRT16, JUP, PTPRM
BP	GO:0051271	negative regulation of cellular component movement	0.015814018	0.014369505	CYP1B1, IGFBP5, DPYSL3, MEOX2, DAB2IP, NRP1, DACH1, KRT16, JUP, PTPRM
BP	GO:0007043	cell-cell junction assembly	0.017748541	0.016127321	CTNND1, TJP1, CDH5, CDH13, GJC1, JUP
BP	GO:0003158	endothelium development	0.01887607	0.017151857	CD34, HEY1, ZEB1, NRP1, TJP1, CDH5
BP	GO:0030336	negative regulation of cell migration	0.022636214	0.020568535	CYP1B1, IGFBP5, DPYSL3, MEOX2, DAB2IP, DACH1, KRT16, JUP, PTPRM
BP	GO:0045766	positive regulation of angiogenesis	0.026799299	0.024351348	CD34, CYP1B1, PLK2, SASH1, NRP1, CDH5, JUP
BP	GO:2,000,146	negative regulation of cell motility	0.02683029	0.024379507	CYP1B1, IGFBP5, DPYSL3, MEOX2, DAB2IP, DACH1, KRT16, JUP, PTPRM
BP	GO:0031290	retinal ganglion cell axon guidance	0.02683029	0.024379507	EFNA5, NRP1, PTPRM
BP	GO:0031589	cell-substrate adhesion	0.02683029	0.024379507	CD34, LIMS2, FN1, FAM107A, EFNA5, NRP1, FERMT2, CDH13, JUP
BP	GO:0007044	cell-substrate junction assembly	0.02683029	0.024379507	FN1, FAM107A, EFNA5, NRP1, FERMT2
BP	GO:0150115	cell-substrate junction organization	0.02683029	0.024379507	FN1, FAM107A, EFNA5, NRP1, FERMT2
BP	GO:0010810	regulation of cell-substrate adhesion	0.026892301	0.024435855	LIMS2, FN1, FAM107A, EFNA5, NRP1, CDH13, JUP
BP	GO:0051017	actin filament bundle assembly	0.026892301	0.024435855	FAM107A, SYNPO, DPYSL3, BAIAP2L1, AIF1L, NRP1
BP	GO:0034446	substrate adhesion-dependent cell spreading	0.027335382	0.024838463	LIMS2, FN1, EFNA5, NRP1, FERMT2
BP	GO:0061572	actin filament bundle organization	0.028586963	0.02597572	FAM107A, SYNPO, DPYSL3, BAIAP2L1, AIF1L, NRP1
BP	GO:0010594	regulation of endothelial cell migration	0.034323026	0.031187828	PLK2, SASH1, MEOX2, DAB2IP, NRP1, JUP, PTPRM
BP	GO:1,904,018	positive regulation of vasculature development	0.034323026	0.031187828	CD34, CYP1B1, PLK2, SASH1, NRP1, CDH5, JUP
BP	GO:0072330	monocarboxylic acid biosynthetic process	0.039658473	0.036035915	PDK4, LPL, IDO1, FABP5, BGN, FADS6, OSBPL1A
BP	GO:0045446	endothelial cell differentiation	0.041833964	0.038012688	HEY1, ZEB1, NRP1, TJP1, CDH5
BP	GO:0048871	multicellular organismal homeostasis	0.04501582	0.040903902	CD34, EPAS1, WWTR1, LDB2, PDK4, FABP5, FABP4, EDNRB, ZNF423, KRT16
BP	GO:0001952	regulation of cell-matrix adhesion	0.047747232	0.043385816	FAM107A, EFNA5, NRP1, CDH13, JUP

(Continued)

**Table 1.** (Continued).

ONTOLOGY	ID	Description	p.adjust	qvalue	geneID
BP	GO:0010811	positive regulation of cell-substrate adhesion	0.049966936	0.045402763	LIMS2, FN1, NRP1, CDH13, JUP
CC	GO:0005925	focal adhesion	8.38E-05	6.67E-05	ENAH, LIMS2, ARHGAP31, FAM107A, EPB41 L2, AIF1L, NRP1, PPFIBP1, FERMT2, SLC9A3R2, CDH13, JUP, TGM2
CC	GO:0030055	cell-substrate junction	8.38E-05	6.67E-05	ENAH, LIMS2, ARHGAP31, FAM107A, EPB41 L2, AIF1L, NRP1, PPFIBP1, FERMT2, SLC9A3R2, CDH13, JUP, TGM2
CC	GO:0030027	lamellipodium	0.000948734	0.000755338	ENAH, FGD5, ARHGAP31, APBB2, DPYSL3, CTNND1, FERMT2, PTPRM
CC	GO:0016342	catenin complex	0.000948734	0.000755338	CTNND1, CDH5, CDH13, JUP
CC	GO:0031252	cell leading edge	0.000948734	0.000755338	ENAH, FGD5, ARHGAP31, FAM107A, LDB2, APBB2, DPYSL3, AIF1L, CTNND1, FERMT2, PTPRM
CC	GO:0005911	cell-cell junction	0.001056975	0.000841514	LIMS2, SYNPO, EFNA5, MPDZ, TMEM47, CTNND1, TJP1, CDH5, GJC1, JUP, PTPRM
CC	GO:0043296	apical junction complex	0.005423338	0.004317806	SYNPO, MPDZ, CTNND1, TJP1, CDH5, JUP
CC	GO:0062023	collagen-containing extracellular matrix	0.015437633	0.012290715	FN1, SPARCL1, EFNA5, BGN, A2M, MGP, CDH13, SERPINB8, TGM2
CC	GO:0005912	adherens junction	0.022320104	0.017770213	EFNA5, TMEM47, CTNND1, JUP
CC	GO:0045177	apical part of cell	0.036690671	0.029211381	CD34, FN1, CLIC5, GPIHBP1, MPDZ, TJP1, SLC9A3R2, ATP8B1
CC	GO:0043292	contractile fiber	0.042863184	0.034125645	TIMP4, SYNPO, IDO1, TNNT3, FERMT2, JUP
CC	GO:0016324	apical plasma membrane	0.042863184	0.034125645	CD34, FN1, CLIC5, GPIHBP1, MPDZ, SLC9A3R2, ATP8B1
CC	GO:0019897	extrinsic component of plasma membrane	0.042863184	0.034125645	CTNND1, FERMT2, CDH5, CDH13, JUP
MF	GO:0045296	cadherin binding	0.000192766	0.000171861	BAIAP2L1, NDRG1, DAB2IP, CTNND1, PPFIBP1, STXBP6, TJP1, SLC9A3R2, CDH5, CDH13, JUP, PTPRM
MF	GO:0050839	cell adhesion molecule binding	0.001248405	0.001113019	FN1, BAIAP2L1, NDRG1, DAB2IP, CTNND1, PPFIBP1, STXBP6, TJP1, SLC9A3R2, CDH5, CDH13, JUP, PTPRM
MF	GO:0098632	cell-cell adhesion mediator activity	0.021225025	0.018923229	BAIAP2L1, DSCAML1, STXBP6, JUP
MF	GO:0008143	poly(A) binding	0.024149341	0.021530411	RBMS3, RBPMS, RBMS2
MF	GO:0098631	cell adhesion mediator activity	0.024149341	0.021530411	BAIAP2L1, DSCAML1, STXBP6, JUP
MF	GO:0070717	poly-purine tract binding	0.03512892	0.031319284	RBMS3, RBPMS, RBMS2
MF	GO:0071813	lipoprotein particle binding	0.03512892	0.031319284	LPL, GPIHBP1, CDH13
MF	GO:0071814	protein-lipid complex binding	0.03512892	0.031319284	LPL, GPIHBP1, CDH13

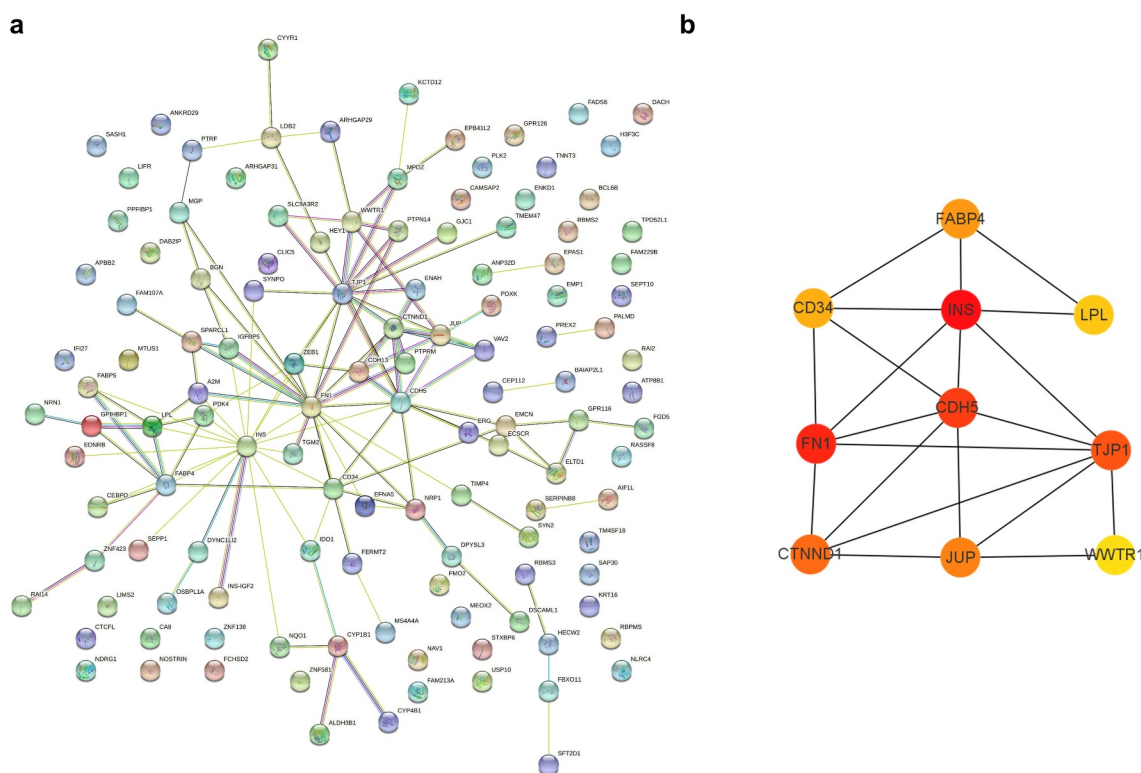
*ARG1* in AMI patients than healthy controls, indicating the clinical significance of *ARG1* in AMI [27]. In our study, the *ARG1* expression in platelets represented the power (with AUC of 0.9, Figure 3a) in identifying patients with STEMI from SCAD, suggesting its potential as a biomarker for distinguishing cardiovascular disease. *NAMPTL*, a pseudogene, was detected to be stimulated in blood or immune cells; *NAMPTL* expression was also observed in heart tissues and showed great performance as a biomarker for separating STEMI and SCAD with an AUC of 0.92. Correlation analysis revealed its significant association with the distribution of neutrophil cells (Figure 3b), indicating its potential as an indicator for immune states of platelets.

Additionally, with WGCNA, we observe one STEMI-related module containing 141 genes

(Figure 4e) involved in biological processes of cell junction, cell migration, cell adhesion, and cell motility (Figure 5). Crucial roles of cell-cell junction participating in the cardiac conduction system have been reported [28]. Robert, et al. found that actin cytoskeleton mediates the secretion of alpha-granule and dense granule [29]; It was believed that  $\alpha$ -granule secretion is associated with platelet activation [30]. Platelet activation, associated with coronary thrombus, plays a crucial role in the development and STEMI [31,32]. Similarly, we observed the significant enrichment of the actin cytoskeleton of STEMI-related genes (Figure 5d), indicating the various roles of platelet activation in STEMI and SCAD. The PPAR signaling pathway, a crossing regulator of lipid signaling and inflammation [33], was enriched, suggesting its crucial role in platelets in response to STEMI (Figure 5d). A previous study found that the

**Table 2.** Enriched KEGG pathways of genes associated with AMI.

ID	Description	p.adjust	qvalue	geneID
hsa03320	PPAR signaling pathway	0.008278213	0.00630721	A0A1B1RVA9, P06858, E7DVW5, Q01469, E7DVW4, P15090
hsa04913	Ovarian steroidogenesis	0.0345036	0.026288457	Q16678, Q53TK1, I3WAC9, P01308
hsa00750	Vitamin B6 metabolism	0.0345036	0.026288457	V9HWC3, O00764
hsa04923	Regulation of lipolysis in adipocytes	0.0345036	0.026288457	E7DVW4, P15090, I3WAC9, P01308
hsa05215	Prostate cancer	0.0345036	0.026288457	B2RB18, P37275, I3WAC9, P01308, P11308
hsa04810	Regulation of actin cytoskeleton	0.049184985	0.037474274	Q8N857, P02751, Q6MZM7, Q9UQS6, P52735, I3WAC9, P01308
hsa04960	Aldosterone-regulated sodium reabsorption	0.049184985	0.037474274	I3WAC9, P01308, Q15599
hsa00982	Drug metabolism – cytochrome P450	0.049184985	0.037474274	Q5JPC7, Q99518, A0A024R5D8, P43353
hsa04360	Axon guidance	0.049184985	0.037474274	Q8N857, P52803, O14786, Q68DN3, Q59F20, Q6AWA9
hsa04520	Adherens junction	0.049184985	0.037474274	O60716, Q6MZU1, Q07157, P28827
hsa00980	Metabolism of xenobiotics by cytochrome P450	0.049184985	0.037474274	Q16678, Q53TK1, A0A024R5D8, P43353
hsa00380	Tryptophan metabolism	0.049184985	0.037474274	Q16678, Q53TK1, P14902
hsa05204	Chemical carcinogenesis	0.049184985	0.037474274	Q16678, Q53TK1, A0A024R5D8, P43353

**Figure 6.** Protein–protein interactions and hub genes of STEMI-related genes. (a) Protein–protein interactions of STEMI-associated genes; (b) represented the top 10 predicted hub genes with Cytoscape software.

downregulation of peroxisome proliferator-activated receptor  $\gamma$  (PPAR $\gamma$ ) contributes to the activation and aggregation, eventually forming micro-thromboses,

which finally leads to myocardial dysfunction [34]. Consistently, we found that genes (associated with platelet activation and involved in the PPAR pathway)

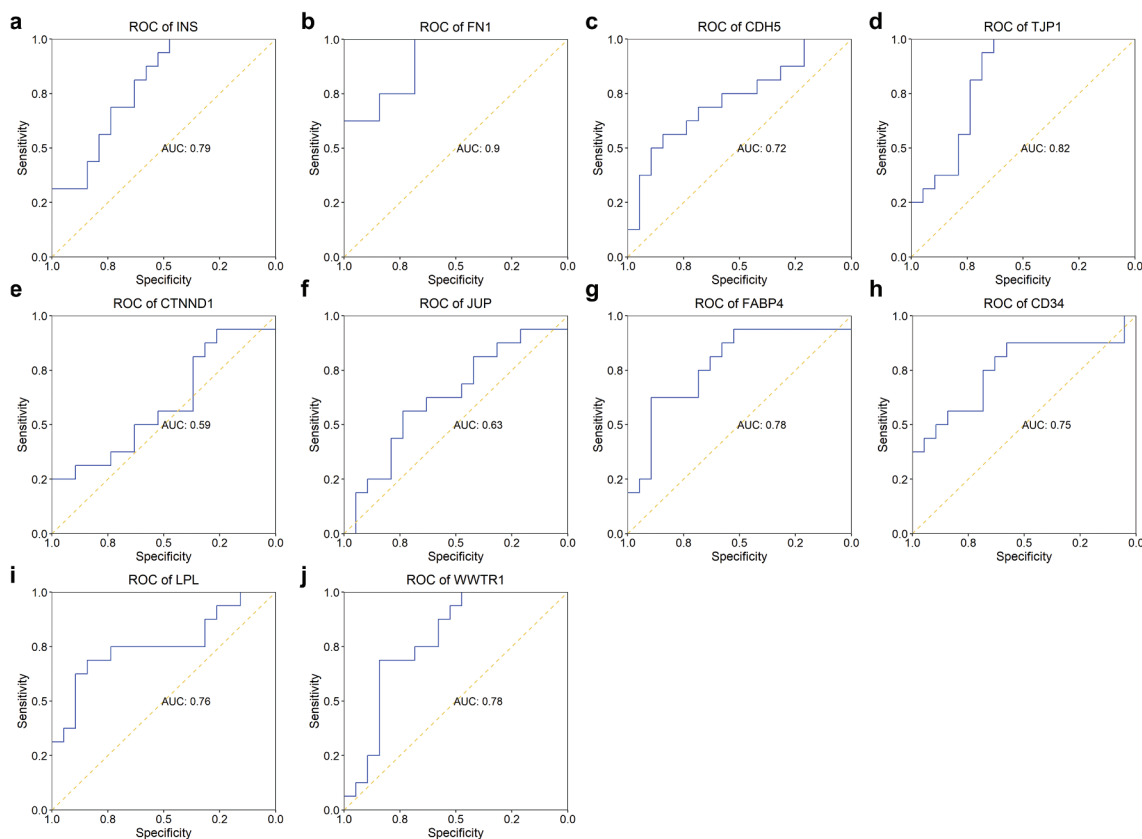


**Figure 7. ROC of hub genes in distinguishing patients with STEMI from healthy controls.** The ability of hub genes as reporters for patients with STEMI was visualized.

showed different expression patterns in STEMI and healthy donors (Figure 4d). Together, these findings indicated the critical roles for platelet activation and the PPAR pathway in the causing of STEMI, enhancing the emergency of anti-inflammation therapy for patients with STEMI.

With PPI, we obtained 10 hub genes from the STEMI-related module; four genes (*FN1*, *CD34*, *LPL*, and *WWTR1*) showed capability as biomarkers for STEMI (Figures 7, 8); *FN1*, encoding fibronectin in plasma, especially, performed well in differentiating patients with STEMI both from healthy donors and patients with SCAD with AUC of 0.9 (Figure 7b) and 0.85 (Figure 8b), respectively. The previous publication reported that the cardiac fibronectin expression was rapidly and considerably increased in the infarcted region of the ventricle, which indicates the critical role of *FN1* in regulating ventricle infarction [35]. However,

we did not observe significantly different expression of *FN1* in patients with STEMI compared to healthy donors or SCAD patients. More experiments need to be conducted to analyze the role of *FN1* in platelets in STEMI.

## Conclusion

In conclusion, with the expression of genes in platelets, we observed different roles of immune states in platelets in response to SCAD and STEMI and first reported the potential of distribution of neutrophils as a molecular signature for separating patients with STEMI from SCAD. We revealed two novel genes (*ARG1* and *NAMPTL*) as biomarkers for identifying STEMI from SCAD; *FN1* shows potential as a novel biomarker for STEMI with great performance in identifying STEMI patients from healthy controls and SCAD patients.

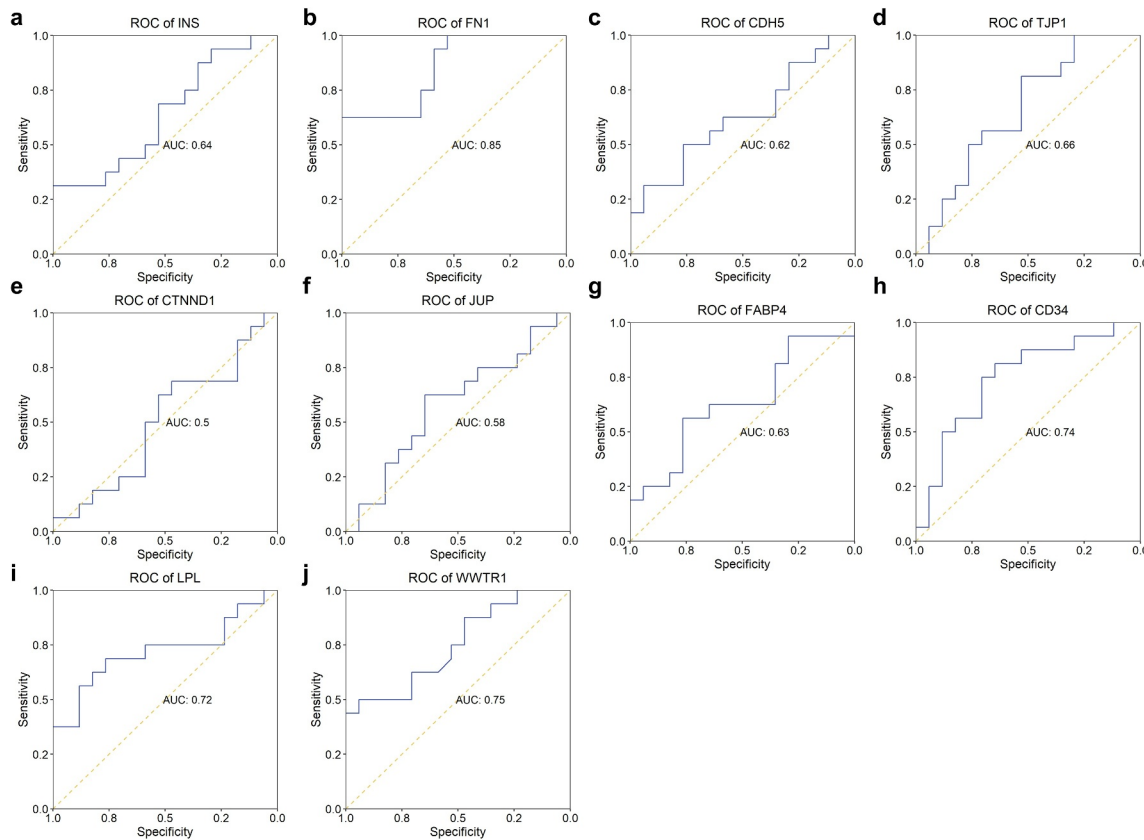


**Figure 8. ROC of hub genes in separating patients with STEMI from SCAD.** The AUC of 10 hub genes in identifying STEMI from SCAD was depicted.

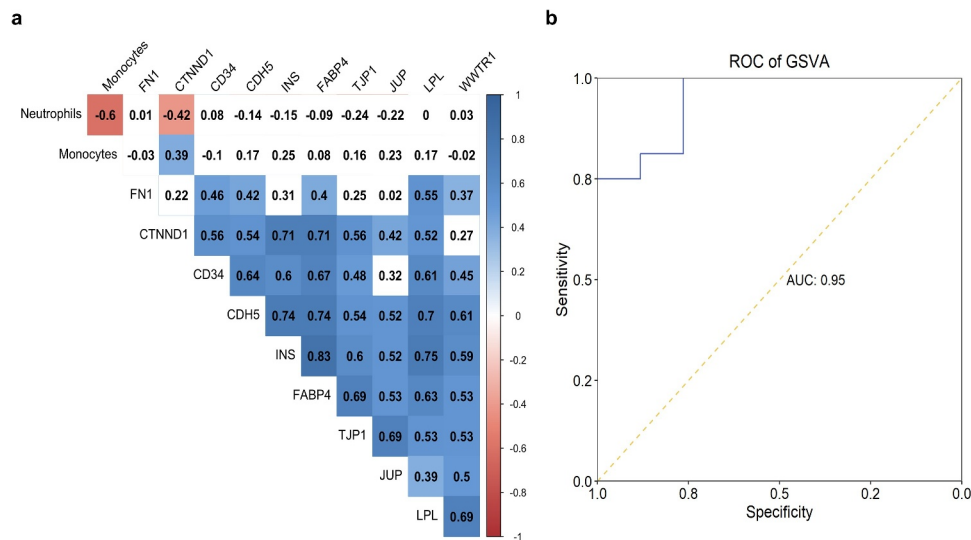


**Figure 9. Correlation of hub genes and distribution of two immune cells.** The correlation table indicated the association of gene expression and fractions of monocytes and neutrophils; the correlation was color-coded from -1 (red) to 1 (blue); association without significance ( $P$ -value > 0.01) was blank. (b) The capability of GSVA index of *ARG1*, *NAMPTL*, and *FN1* expression and neutrophils distribution in identifying patients with STEMI from SCAD was depicted.

## Acknowledgements

None.

## Availability of data and material

The datasets used and/or analyzed during the current study are available from the corresponding author on reasonable request.

## Disclosure statement

The authors declare there are no competing interests.

## Funding

This work was supported by grants from Zhejiang Medical and Health Science and Technology Plan Project (2021KY242) and Traditional Chinese Medical science and technology plan of Zhejiang Province (2019ZB099); Traditional Chinese Medical science and technology plan of Zhejiang Province [2019ZB099].

## Author contributions

Study design: Yun Xie

Data collection: Yi Wang

Data analysis: Linjun Zhao

Interpretation of data: Fang Wang

Draft manuscript: Yun Xie

Review manuscript: Jinyan Fang

## ORCID

Jinyan Fang  <http://orcid.org/0000-0002-4084-8255>

## References

- [1] Wang C, Jing Q. Non-coding RNAs as biomarkers for acute myocardial infarction. *Acta Pharmacol Sin.* 2018;39(7):1110–1119.
- [2] Yang EH, Brilakis ES, Reeder GS, Gersh BJ. Modern management of acute myocardial infarction. *Curr Probl Cardiol.* 2006;31(12):769–817.
- [3] Reed GW, Rossi JE, Cannon CP. Acute myocardial infarction. *Lancet.* 2017;389(10065):197–210.
- [4] Braunwald E. Unstable angina and non-ST elevation myocardial infarction. *Am J Respir Crit Care Med.* 2012;185(9):924–932.
- [5] Healy AM, Pickard MD, Pradhan AD, Wang Y, Chen Z, Croce K, et al. Platelet expression profiling and clinical validation of myeloid-related protein-14 as a novel determinant of cardiovascular events. *Circulation.* 2006;113(19):2278–2284.
- [6] McManus DD, Beaulieu LM, Mick E, Tanriverdi K, Larson MG, Keaney JF, Jr., et al. Relationship among circulating inflammatory proteins, platelet gene expression, and cardiovascular risk. *Arterioscler Thromb Vasc Biol.* 2013;33(11):2666–2673.
- [7] Davies MJ, Thomas A. Thrombosis and acute coronary-artery lesions in sudden cardiac ischemic death. *N Engl J Med.* 1984;310(18):1137–1140.
- [8] Bonaventura A, Montecucco F, Dallegri F, Carbone F, Luscher TF, Camici GG, et al. Novel findings in neutrophil biology and their impact on cardiovascular disease. *Cardiovasc Res.* 2019;115(8):1266–1285.
- [9] Westman PC, Lipinski MJ, Luger D, Waksman R, Bonow RO, Wu E, et al. Inflammation as a driver of adverse left ventricular remodeling after acute myocardial infarction. *J Am Coll Cardiol.* 2016;67(17):2050–2060.
- [10] Sreejit G, Abdel-Latif A, Athmanathan B, Annabathula R, Dhyani A, Noothi SK, et al. Neutrophil-derived S100A8/A9 amplify granulopoiesis after myocardial infarction. *Circulation.* 2020;141(13):1080–1094.
- [11] Ren Z, Yang K, Zhao M, Liu W, Zhang X, Chi J, et al. Calcium-sensing receptor on neutrophil promotes myocardial apoptosis and fibrosis after acute myocardial infarction via NLRP3 inflammasome activation. *Can J Cardiol.* 2020;36(6):893–905.
- [12] Eghbalzadeh K, Georgi L, Louis T, Zhao H, Keser U, Weber C, et al. Compromised anti-inflammatory action of neutrophil extracellular traps in PAD4-deficient mice contributes to aggravated acute inflammation after myocardial infarction. *Front Immunol.* 2019;10:2313.
- [13] Horckmans M, Ring L, Duchene J, Santovito D, Schloss MJ, Drechsler M, et al. Neutrophils orchestrate post-myocardial infarction healing by polarizing macrophages towards a reparative phenotype. *Eur Heart J.* 2017;38(3):187–197.
- [14] Ritchie ME, Phipson B, Wu D, Hu Y, Law CW, Shi W, et al. limma powers differential expression analyses for RNA-sequencing and microarray studies. *Nucleic Acids Res.* 2015;43(7):e47.
- [15] Langfelder P, Horvath S. WGCNA: an R package for weighted correlation network analysis. *BMC Bioinformatics.* 2008;9(1):559.
- [16] Yu G, Wang LG, Han Y, He QY. clusterProfiler: an R package for comparing biological themes among gene clusters. *OMICS.* 2012;16(5):284–287.
- [17] Hanzelmann S, Castelo R, Guinney J. GSEA: gene set variation analysis for microarray and RNA-seq data. *BMC Bioinformatics.* 2013;14(1):7.
- [18] Frossard M, Fuchs I, Leitner JM, Hsieh K, Vlcek M, Losert H, et al. Platelet function predicts myocardial damage in patients with acute myocardial infarction. *Circulation.* 2004;110(11):1392–1397.
- [19] Stojkovic S, Nossent AY, Haller P, Jager B, Vargas KG, Wojta J, et al. MicroRNAs as regulators and biomarkers of platelet function and activity in coronary artery disease. *Thromb Haemost.* 2019;119(10):1563–1572.

- [20] Capodanno D, Angiolillo DJ. Antithrombotic therapy for atherosclerotic cardiovascular disease risk mitigation in patients with coronary artery disease and diabetes mellitus. *Circulation*. 2020;142(22):2172–2188.
- [21] Gadi I, Fatima S, Elwakiel A, Nazir S, Al-Dabet MM, Rana R, et al. Different DOACs control inflammation in cardiac ischemia-reperfusion differently. *Circ Res*. 2020;128(4):513–529.
- [22] Luscher TF. The sooner, the better: anti-inflammation in acute myocardial infarction. *Eur Heart J*. 2020;41(42):4100–4102.
- [23] Dai Y, Chen Y, Wei G, Zha L, Li X. Ivabradine protects rats against myocardial infarction through reinforcing autophagy via inhibiting PI3K/AKT/mTOR/p70S6K pathway. *Bioengineered*. 2021;12(1):1826–1837.
- [24] von Hundelshausen P, Weber C. Platelets as immune cells: bridging inflammation and cardiovascular disease. *Circ Res*. 2007;100(1):27–40.
- [25] Silvestre-Roig C, Braster Q, Ortega-Gomez A, Soehnlein O. Neutrophils as regulators of cardiovascular inflammation. *Nat Rev Cardiol*. 2020;17(6):327–340.
- [26] Gobbi G, Carubbi C, Tagliazucchi GM, Masselli E, Mirandola P, Pigazzani F, et al. Sighting acute myocardial infarction through platelet gene expression. *Sci Rep*. 2019;9(1):19574.
- [27] Zhang R, Ji Z, Qu Y, Yang M, Su Y, Zuo W, et al. Clinical value of ARG1 in acute myocardial infarction patients: Bioinformatics-based approach. *Biomed Pharmacother*. 2020;121:109590.
- [28] Mezzano V, Sheikh F. Cell-cell junction remodeling in the heart: possible role in cardiac conduction system function and arrhythmias? *Life Sci*. 2012;90(9–10):313–321.
- [29] Flaumenhaft R, Dilks JR, Rozenvayn N, Monahan-Earley RA, Feng D, Dvorak AM. The actin cytoskeleton differentially regulates platelet alpha-granule and dense-granule secretion. *Blood*. 2005;105(10):3879–3887.
- [30] Brydon L, Magid K, Steptoe A. Platelets, coronary heart disease, and stress. *Brain Behav Immun*. 2006;20(2):113–119.
- [31] Silvain J, Collet JP, Nagaswami C, Beygui F, Edmondson KE, Bellemain-Appaix A, et al. Composition of coronary thrombus in acute myocardial infarction. *J Am Coll Cardiol*. 2011;57(12):1359–1367.
- [32] Calvieri C, Tanzilli G, Bartimoccia S, Cangemi R, Arrivi A, Dominici M, et al. Interplay between oxidative stress and platelet activation in coronary thrombus of STEMI patients. *Antioxidants (Basel)*. 2018;7(7).
- [33] Wahli W, Michalik L. PPARs at the crossroads of lipid signaling and inflammation. *Trends Endocrinol Metab*. 2012;23(7):351–363.
- [34] Zhou H, Li D, Zhu P, Hu S, Hu N, Ma S, et al. Melatonin suppresses platelet activation and function against cardiac ischemia/reperfusion injury via PPARgamma/FUNDC1/mitophagy pathways. *J Pineal Res*. 2017;63.
- [35] Knowlton AA, Connelly CM, Romo GM, Mamuya W, Apstein CS, Brecher P. Rapid expression of fibronectin in the rabbit heart after myocardial infarction with and without reperfusion. *J Clin Invest*. 1992;89(4):1060–1068.